GEOLOGICA CARPATHICA, OCTOBER 2022, 73, 5, 473–484 https://doi.org/10.31577/GeolCarp.73.5.5

Influence of fluid flows on low-temperature thermochronology: An example from the Podhale Basin, Internal Western Carpathians, Poland

FRANCISCO SANCHEZ NASSIF[1,✉], FEDERICO M. DÁVILA[1], ADA CASTELLUCIO[2], GILDA COLLO[1] and ANDRES MORA[3]

[1]Centro de Investigaciones en Ciencias de la Tierra (Cicterra), Cordoba, Cordoba, Argentina; ✉nassif.franciscosanchez@gmail.com
[2]Department of Geosciences, University of Padua, Padua, Italy; currently at Edison Exploration & Production S.p.A, Milan, Italy
[3]Ecopetrol, Botafogo, Rio de Janeiro, Brazil

(Manuscript received August 20, 2021; accepted in revised form August 30, 2022; Associate Editor: Jacek Grabowski)

Abstract: A novel approach that couples hydrological and thermochronological modelling is tested in a well-known hydrothermal system, the Inner Western Carpathians, providing insights of the yet-unexplained Apatite Fission Track (AFT) ages of the Podhale Basin. Our new model improves previous ones by incorporating the effects of fluid circulation, by considering compaction, smectite dehydration and meteoric water as sources of fluid. Rock properties such as thermal diffusivity, porosity and permeability, are dependent on lithology and the effective-stress state of the system, making our calculations depart from previous efforts on thermochronological modelling. Particularly, we examined young (around 12 Ma) apatite fission track ages from Oligocene strata of the Podhale wild flysch, which suggest the occurrence of either substantial burial or an elevated basal thermal paleogradient, even though none of the above have been documented in the area. Such problem is addressed on this contribution, since by reproducing previous numerical experiments but adding groundwater circulation this time, improved thermally-reset AFT ages of the Podhale Basin are obtained. Thermal, hydrological and mineralogical observations are successfully reproduced, putting forward the calibration and validity of the model here proposed. Furthermore, our findings not only unveil the linking between the hydrological and thermal phenomena present in the study region, but also, trigger new questions on the processes that should be taken into account when thermochronological calculations are concerned.

Keywords: thermochronological modelling, Podhale Basin, fluid flow

Introduction

Low-temperature thermochronological modelling have cast some light on the relationship between tectonics and thermal evolution (e.g., Braun 2003; Braun & Willett 2013). Even though it has provided valuable insights for different geodynamic scenarios (Braun 2016; Łuszczak et al. 2017; Margirier et al. 2018; Georgieva et al. 2019; Parks & McQuarrie 2019), the conceptual framework it is built upon still requires to incorporate other key parameters (e.g., fluid flows) than those related to burial and exhumation processes (e.g., isostasy, rock uplift, erodibility parameters or pluvial precipitation). The present study concerns the influence of water circulation on the thermal field and the resultant thermochronological ages, by considering the Internal Western Carpathians (cf. Hók et al. 2014) of Poland as a natural laboratory. Interestingly such an influence, although discussed in previous research efforts (Deming 1994; Ge & Garven 1992), has not been addressed by numerical thermochronological models in the Western Carpathians (see Castelluccio et al. 2015 for latest results).

Latest works on low-temperature thermochronological modelling have been crucial to the assessment of time–temperature histories of apatite and zircon grains (Ketcham 2005; Gallagher 2012), deformation and landscape evolution (Braun 2003; Braun & Willett 2013), and, lately, to improve kinematic restorations (Almendral et al. 2015; Parks & McQuarrie 2019). Efforts on the latter have been tested in structurally complex settings such as the Andes and the Alps–Carpathian Cordilleran thrust belts (Mora et al. 2015; Castelluccio et al. 2015), providing valuable insights for tying thrusting kinematics to cooling ages. Nonetheless, these contributions are still limited, given that they assume thrusting in a "dry" scenario despite that relevance of fluid circulation has been broadly noted (Forster & Smith 1989; Nemčok et al. 2009). Indeed, modelling of subduction zones (e.g., Van Keken et al. 2002; Coussens et al. 2018), where most fluid flow modelling attempts have been carried out, have demonstrated that pore pressure and the associated fluid movement can promote substantial modifications on the seismicity and thermal state of a geological system. Towards the foreland, the situation is alike, with the stress and thermal regimes being conditioned by the presence of water (Davis et al. 1983; Jessop & Majorowicz 1994; Cobbold et al. 2004; Hardebol et al. 2009). Given the structural complexity of foreland fold-and-thrust-belts, the extent of heat advection by groundwater circulation is less constrained in such scenarios, making them exemplary sites for enhancing our understanding of deformed systems. Following

this, the Inner Western Carpathians in Poland thrust belt constitutes an ideal zone, since not only fluid flow has been extensively documented, but also thermal and thermochronological data are abundant (Sokołowski 1993; Anczkiewicz et al. 2013; Castelluccio et al. 2015). In fact, previous thermokinematic efforts in the region (e.g., Castelluccio et al. 2015) could not fit locally the structural reconstructions with AFT data (observed and modelled), likely because they did not consider hydrothermalism in the numerical modelling. By taking into account groundwater movement, the present work seeks to reproduce AFT ages at the hydrothermally-influenced Podhale Basin, furthermore testing if groundwater circulation affects or not low-temperature thermochronological ages.

In this contribution we model the thermal and fluid flow evolution of the Podhale Basin in the Internal Western Carpathians (see Fig. 1) by integrating structural kinematic restorations (Castelluccio et al. 2015) with thermochronometric data. In our computations, we considered a modified version of Almendral et al. (2015) code, which incorporated piezometric-head and related constitutive-relationship equations (see Sanchez et al. 2021). Basically, Darcy velocities, obtained from a mass balance formulation, were coupled with thermal equations. In addition, we also modelled and compared the thermally-induced smectite-to-illite reaction (Huang et al. 1993). This process allowed us to estimate the amount of water released by clay dehydration, which plays a primary role in subduction margins (Lauer & Saffer 2015; Spinelli et al. 2006) and foreland scenarios (Gonzalez-Penagos et al. 2014), and is suggested to be of major importance in the study region given the substantial amount of claystones present (Porowski 2014, 2015). Unlike previous thermochronological models, ours is calibrated with thermal, hydrological and mineralogical data (Sokołowski 1993; Chowaniec & Poprawa 1998; Marynowski et al. 2005; Środoń et al. 2006); which puts forward the benefits and the validity of the comprehensive model here considered.

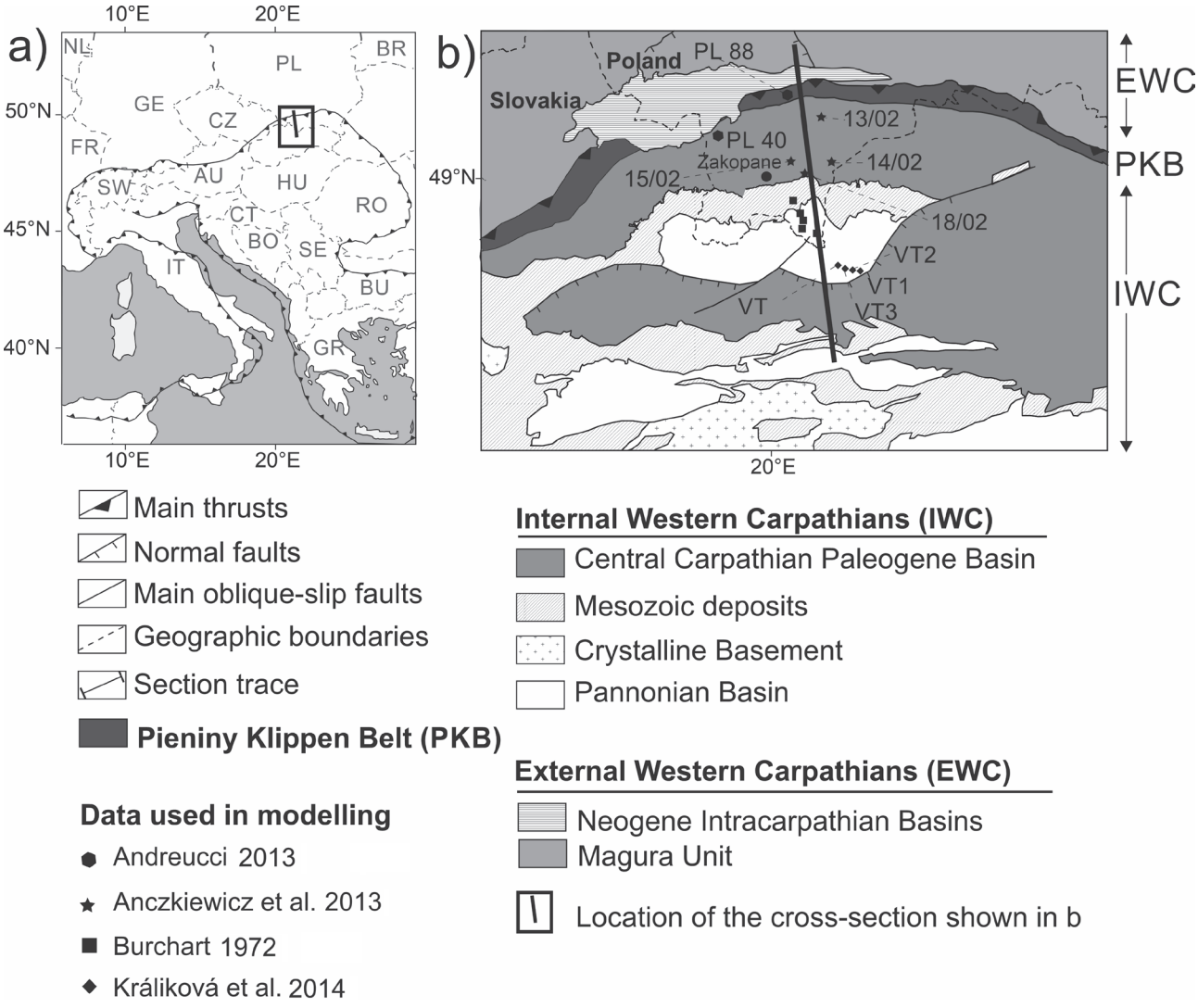

Fig 1. Location of the study area (**a**) and geological map of the IWC region (**b**). The thick black line illustrated inside the black square in (a), as well as the same black line in (b), represent the position of the cross-section depicted in Figure 3.

Geological setting and thermal state

The study region is located in the Internal Western Carpathian (IWC), in the northern part of the Alpine–Carpathian orogenic system (Fig. 1a, b). Three main geological units compound this region, from south to north: The Tatra Mountains, Podhale Basin, and Pieniny Klippen Belt. The Podhale Basin is a prolific hydrothermal intramontane depocenter, interpreted as a wedge-top basin by Castelluccio et al. (2015), and constitutes the main objective of this contribution (see Figs. 1, 2 and 3). The Tatra Mts. represents the main core of the Carpathian thrust belt and form an asymmetrical horst-like W–E trending mega-anticline (Králiková et al. 2014). The Pieniny Klippen belt, in turn, is a major geological boundary interpreted as an ancient suture belt (Maheľ 1981) that separates the Internal and External Western Carpathians (see Figs. 1, 3) and (as shown below), the groundwater systems in the region (Chowaniec 2004, 2009). Broadly, the IWC is formed by an Upper Paleozoic basement, covered by Mesozoic and Cenozoic sedimentary successions, deformed in five major compressional events (see Pešková et al. 2009; Vojtko et al. 2010; Castelluccio et al. 2015; Śmigielski et al. 2012). The major shortening episode would have occurred at approximately 30 Ma (Oligocene), which is the time when our modelling starts. Our model is based on the palinspastic reconstructions and basin evolution proposed by Castelluccio et al. (2015).

AFT and AHe (Apatite Helium) samples (see Castelluccio et al. 2015) across the IWC (see Fig. 1b) have elucidated the thermal evolution of the study region. Cooling ages in

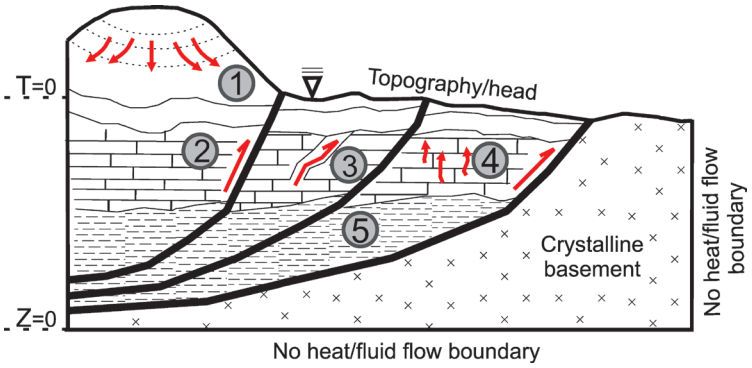

Fig. 2. Model setup illustrating fluid flow processes considered in the model. 1 – Topography-driven flow; 2 – Channelized fluid flow through fault planes; 3 – Fluid circulation through fractures; 4 – Compaction-driven flow; 5 – Clay dewatering. T and Z stand for temperature and depth, respectively.

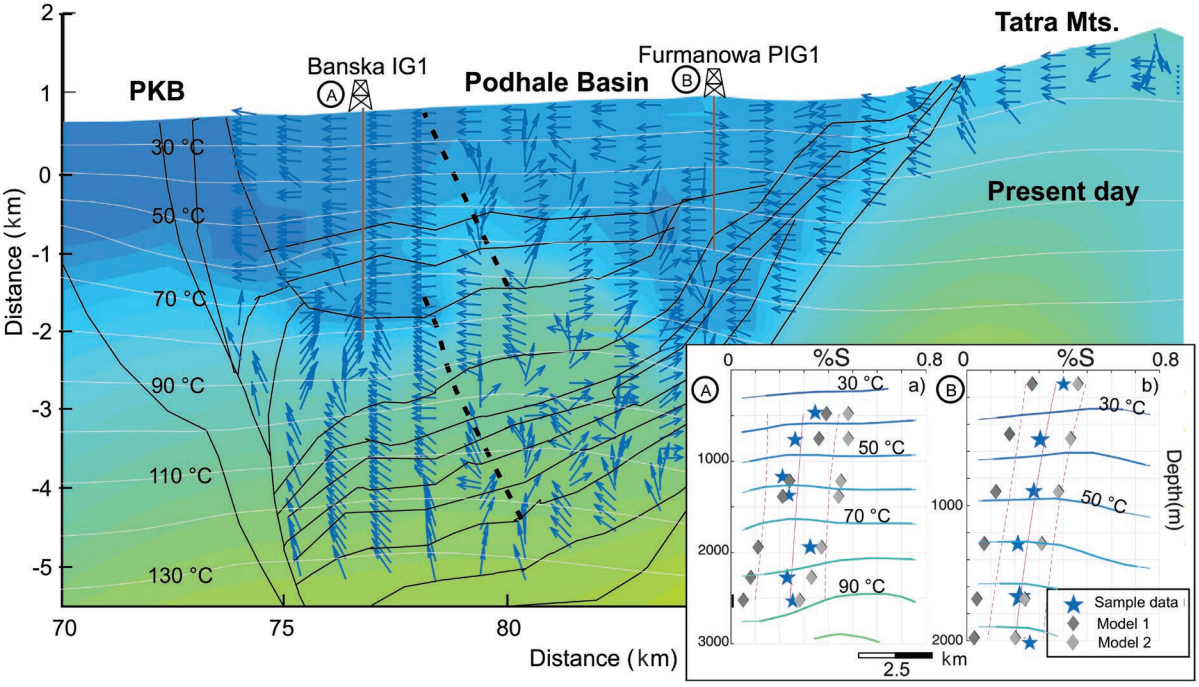

Fig. 3. Model calibration results. Blue arrows represent normalized fluid flow directions, according to piezometric head potential (kKm) depicted as colour scale (right). Dashed lines represent main fracture zones, after Kępińska (2004). Inset figure shows I/S modelling results at Banska IG1 and Furmanowa PIG1 boreholes in the Podhale Basin, as well as the isotherm distribution nearby them with respective distance scale (bottom of inset).

the Podhale Basin are between 11–8 Ma (Anczkiewicz et al. 2013), which are considerably younger than the Eocene to Oligocene depositional ages (Samuel & Fusán 1992; Voigt et al. 2008). Such youngening (thermal resetting) was associated with mantle upwelling and basin subsidence episodes occurred in the Mid-Miocene (Danišík et al. 2012). The aforementioned agrees with vitrinite reflectance and illite–smectite studies, which postulated high paleogeothermal gradients (30 °C/km to 40 °C/km) during the late Miocene evolution of the Podhale Basin (see Danišík et al. 2012; Marynowski & Gaweda 2005). This regional heating is consistent with near-surface geothermal gradient values of 25 °C/km to 35 °C/km supplied from well-log measurements, ascribed to major hydrothermal circulation (Chowaniec & Poprawa 1998; Anczkiewicz et al. 2013). Nonetheless, interstratified clay-mineral analysis from Środoń et al. (2006) has suggested that paleogeothermal gradients would have been much lower, between 20–25 °C/km, implying a substantial unroofing (approximately 6 km) to account for the reported cooling ages. Similar low paleogeothermal gradients (around 20 °C/km) were proposed by Andreucci (2013) and Świerczewska (2005), values considered by Castelluccio et al (2015) in their thermo-kinematic modelling. As mentioned previously, even though such ancient gradients reproduced the cooling ages outside the Podhale Basin (Castelluccio et al. 2015), thermally-reset AFT ages inside the hydrothermal depocenter still remain to be explained. Also, these low geothermal gradients are not compatible with the remarkably high values measured in-situ by water wells (Anczkiewicz et al. 2013; Kępińska 2006). These observations suggest that additional processes might have interfered with burial and exhumation history occurred during the formation of the Carpathian thrust belt. This work focuses particularly on heat convection related to groundwater circulation derived from different sources.

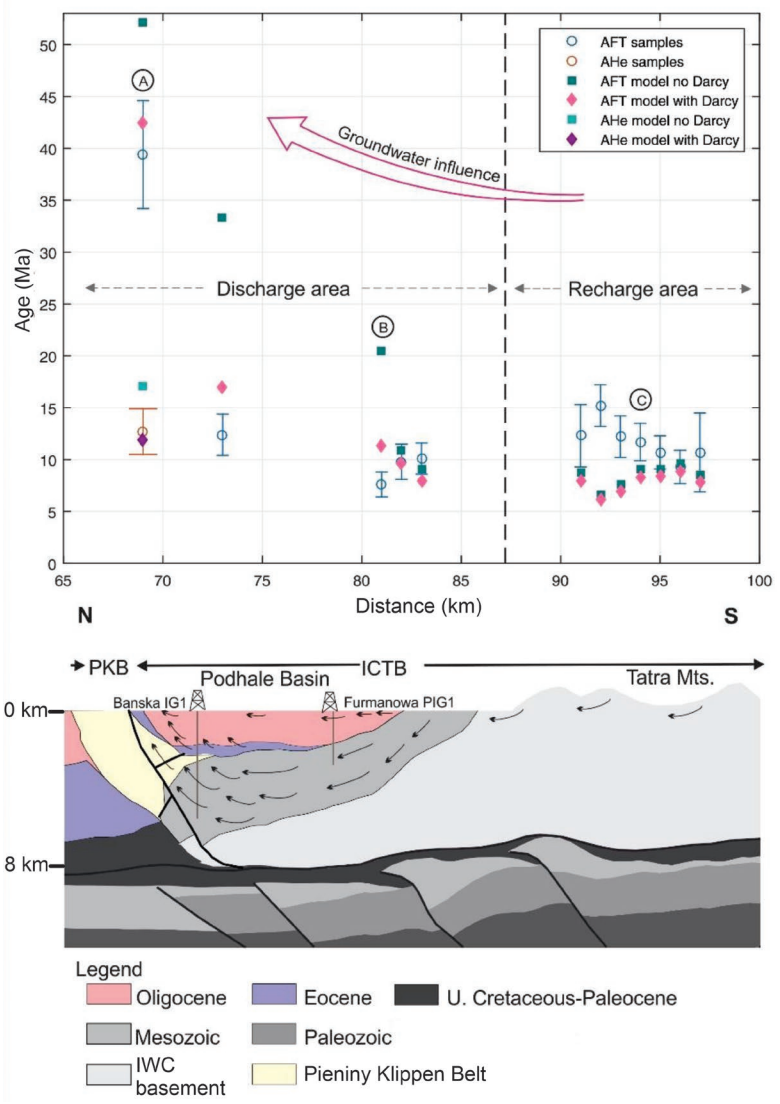

Fig 4. Thermochronological modelling results (above) and simplified structural section (below), with arrows representing documented groundwater flow (Chowaniec & Poprawa 1998; Kępińska 2004). AFT and AHe stand for Apatite Fission Track and Apatite Helium, respectively. AFT samples after Anczkiewicz et al. (2013) and AHe samples after Andreucci (2013).

The hydrogeology of the Polish part of IWC have been extensively studied, as several geothermal aquifers have been recognised in the Podhale Basin (Kępińska 2006; Chowaniec 2009). The recharge area, the aquifer rocks and the impermeable barrier are given by the Tatra Mountains, the Podhale Basin and the Pieniny Klippen Belt, respectively (see Figs. 1, 3 and 4). In the basin, the most important aquifers are the Eocene carbonates and Jurassic marls and limestones (Kępińska 2004). High artesian outflows, associated to a system of connected fractures, have been reported in Zakopane and Banska areas (80 m^3/h and 60 m^3/h, respectively). Isotopic and chemical composition of thermal waters points to a mixed origin, being a complex mixture of meteoric and subsurficial waters (Porowski 2014, 2015; Kępińska 2004, 2006).

Model overview

We used a new version of the finite element code Fetkin (developed and provided by Ecopetrol, see Almendral et al. 2015), recently modified by Sanchez et al. (2021), to simulate unsteady heat and fluid transport along a 30 km, N–S transect through the Podhale Basin that covers both the recharge (Tatra Mountains) and discharge (Podhale flysch sediments) areas (Castelluccio et al. 2015). Simplified lithological characterization of the regions considered is shown in Table 1 (see Castelluccio et al. 2015). Two contrasting models were run for

Table 1: Simplified lithological characterization of the study region.

	Tatra Mts.	Podhale Basin	Pieniny Klippen Belt
Miocene		shales	
Oligocene	shales	shales	
Eocene			
Upper Cretaceous–Paleocene			sandstone, shale
Lower Cretaceous	limestones	limestones	
Jurassic	limestones	limestones	limestones
Triassic	basement	basement	basement
Paleozoic	basement	basement	basement
Basement	basement	basement	basement

comparison: with (fluid model or FM) and without (no fluid model or NFM) fluid flow, representing the former the model proposed by (Sanchez et al. 2021), and the latter the kinematically-based models used to date. To couple hydrological and thermal calculations, a convective term to the diffusion–advection heat equation was added

$$\frac{\partial u}{\partial t} - \nabla\cdot(m\nabla u) + \nabla u\cdot(v_f + v_r) = 0\,, \tag{1}$$

where u is temperature, m thermal diffusivity, and V_f and V_r are fluid and rock velocities, respectively. Darcian fluid velocities were obtained from the gradient in piezometric head present in the system

$$v_f = -k\nabla h\ , \tag{2}$$

where k is hydraulic conductivity and h piezometric potential. Porosities were calculated from Terzagui's effective stress (σ'), considering a lithology-dependent compaction parameter (c)

$$\phi(\sigma') = \phi_{\min} + (\phi_0 - \phi_{\min})e^{-(c\sigma')}\,, \tag{3}$$

where $\phi_{\min}$ and $\phi_{\min}$ are the minimum porosity considered and the lithology-dependent initial porosity, respectively (see Table 2). A $_{\min}$= 0.03 was established. Kozeny-Carman relationships were chosen to calculate rock permeability from the time and space sensitive porosity. Although secondary porosity and permeability have been reported in the basin, they were not taken into account given the uncertainty in the distribution of fractures within the sediments. Porosity-dependent thermal conductivities were derived from

$$K = K_r^{(1-\phi)} K_w^{\phi}\,, \tag{4}$$

where K represents the effective thermal conductivity, K_r lithology-conditioned rock conductivity and K_w thermal conductivity of water, which was assumed constant (see Table 2).

The heat and piezometric head equations were formulated under a fixed Eulerian grid, constructed from the topographic surface down to the bottom of the user-specified grid (Fig. 2). Considered sources of water are shown in Fig. 2. Elevation head (z) was set to 0 along the model bottom, where a fixed temperature (and thus, a thermal gradient) is specified by the user. A time-varying Dirichlet condition was set along the topography, which forced the piezometric head to be equal to the elevation head, as no pore pressure would develop on the surface. Temperature along topography nodes was obtained considering a fixed atmospheric gradient, and was set up as boundary condition as well. A no-flow condition was imposed for model sides and bottom. Fluid flow velocities along fault planes were prescribed, and held constant throughout the simulation (Table 2). Nodes along today's main fracture zones (Kępińska 2004) were also assigned a constant fault permeability. The model evolves from an initial configuration in which the system is considered to be hydrostatic and temperature varies linearly with depth. Then, the computer program obtains the unsteady thermal and hydrological architecture as it evolves from the beginning of the tectonic evolution (see Castelluccio et al. 2015) until present day. We considered Castelluccio et al. (2015) thrusting kinematics, as their proposed structural model successfully reproduced thermochronological ages outside the hydrothermal Podhale Basin.

In order to estimate the amount of water released by clay dehydration, the degree of smectite-to-illite diagenesis was modelled considering the widely-used model of Huang et al. (1993)

$$-\frac{dS}{dt} = A.e^{(-E_a/Ru)}\left[K^+\right]S^2\,, \tag{5}$$

where S is the volumetric smectite content, E_a is the energy of activation, u the temperature, R the gas constant, A the frequency factor, and K the potassium concentration in the solution (see Table 2). Moreover, the volume of water freed from the dehydration reaction was obtained via

$$\gamma = \frac{dS}{dt} HC(1-\phi)\,, \tag{6}$$

where H is the water content in smectite (20 %wt) and C is the volume fraction of I/S in the bulk sediment. C was considered to be 0.65 for shaly rocks, based on bulk XRD analysis from Środoń et al. (2006; ∑2:1). Fluid release from sediment compaction was obtained analogously.

The I/S relationship was modelled in two wells (see location in Figs. 3 and 4). Based on measured mineralogical contents (Środoń et al. 2006), and taking into account studies on I/S evolution that propose a 4-fold variation in potassium (K) concentrations (Roberson & Lahann 1981; Cuadros 2006), two K contents were taken into account for the calcareous-rich sediments of both wellbores. Hence, we considered two K fractions, k=0.00052 ppm (model 1) and k=0.000052 ppm (model 2). Such K fractions were allowed to vary with depth, as well data (Środoń et al. 2006) suggests that potassium availability was not constant throughout the well. Finally, model calibration was performed by taking into account hydrological, thermal, and mineralogical (I/S %) measurements across the Podhale Basin (see Geological setting), as discussed below.

Table 2: Parameters used in modelling scenarios.

Parameter	Value	Units	Reference
Water density	1040	kg/m^3	
Water content in smectite	0.4	Volume Fraction	(Saffer et al. 2008)
Smectite content in clay rock	0.65	Volume Fraction	
Fault permeability	1.00E-20	m^2	(Evans et al. 1997; López & Smith 1996)
Limestone compaction parameter	0.049	1/MPa	(Hantschel & Kaureauf 2009)
Basement compaction parameter	0.0001	1/MPa	(Hantschel & Kaureauf 2009)
Shale compaction parameter	0.096	1/MPa	(Hantschel & Kaureauf 2009)
Sandstone_shale compaction parameter	0.026	1/MPa	(Hantschel & Kaureauf 2009)
Limestone initial porosity	0.51	Volume Fraction	(Hantschel & Kaureauf 2009)
Basement initial porosity	0.05	Volume Fraction	(Hantschel & Kaureauf 2009)
Shale initial porosity	0.7	Volume Fraction	(Hantschel & Kaureauf 2009)
Sandstone_shale initial porosity	0.4	Volume Fraction	(Hantschel & Kaureauf 2009)
Limestone density	2740	kg/m^3	(Hantschel & Kaureauf 2009)
Basement density	2650	kg/m^3	(Hantschel & Kaureauf 2009)
Shale density	2700	kg/m^3	(Hantschel & Kaureauf 2009)
Sandstone_shale density	2760	kg/m^3	(Hantschel & Kaureauf 2009)
Limestone thermal conductivity	3	W/mK	(Hantschel & Kaureauf 2009)
Basement thermal conductivity	2.6	W/mK	(Hantschel & Kaureauf 2009)
Shale thermal conductivity	1.64	W/mK	(Hantschel & Kaureauf 2009)
Sandstone_shale thermal conductivity	3.35	W/mK	(Hantschel & Kaureauf 2009)
Water thermal conductivity	0.64	W/mK	(Hantschel & Kaureauf 2009)
Limestone specific heat	835	J/kgK	(Hantschel & Kaureauf 2009)
Basement specific heat	800	J/kgK	(Hantschel & Kaureauf 2009)
Shale specific heat	860	J/kgK	(Hantschel & Kaureauf 2009)
Sandstone_shale specific heat	860	J/kgK	(Hantschel & Kaureauf 2009)
Water specific heat	4186	J/kgK	(Bear & Verrujit 2012)
Bottom of the model	12	Km	
Temperature along bottom	240	°C	
Temperature along surface	25	°C	
A(frecuency factor for smectite reaction)	8.08E-04	1/seg	(Huang et al. 1993)
E_a	28	kcal/mole	(Huang et al. 1993)

Results

Model calibration

Geothermal gradients at Banska IG1 and Furmanowa PIG1 wells generated by our simulation (23 °C/km and 19 °C/km, respectively, see Fig. 3) are consistent with in-situ temperature measurements (22 °C/km and 14 °C/k, respectively; see Sokołowski 1993). In fact, positive anomalies of 80–100 °C at 2–3 km depth, which represent higher temperatures than those resulting from the basal geothermal gradient (see Kępińska 2004; 18 °C/km in our numerical model), were also satisfactorily reproduced. Reported surface temperature anomalies of around 3 °C next to the PKB (Pomianowski 1988) were not recreated, given the Dirichlet boundary condition imposed along the topographic line. However, the remarkable similarity between wellbore-based spatial distribution of isotherms (Kępińska 2004), and the one rendered by our model, prompts forward the plausibility of the thermal calculations herein presented.

Modelled direction of groundwater flow through the IWC (depicted as arrows in Fig. 3) as a response to the hydrological architecture of the region, is also consistent with observations shown in literature (Chowaniec & Poprawa 1998; see Figs. 3 and 4). The high relief of the Tatra Mts. forms topography-driven flow, which infiltrates in the basin substratum. Hereon the fluid, driven by the piezometric head gradient (Fig. 3), travels throughout the basin until it reaches an impermeable barrier (PKB in Figs. 1 and 3; in almost hydrostatic equilibrium). We remark that even though secondary porosity and permeability (shown to exert a substantial influence on the hydrological regime, Sowiżdżał & Semyrka 2016; Chowaniec 2004) were not considered in this study, the modelled piezometric head field reproduces satisfactorily the first-order hydrological architecture of the basin (Chowaniec & Poprawa 1998; Operacz & Chowaniec 2018). Low primary porosity values obtained in the Oligocene strata (around 7 %, see Fig. 5) are in the range of values reported (Sowiżdżał & Semyrka 2016), which also sustains the validity our calculations. Moreover, the topography and compaction driven flows generated by our results, especially at the Podhale Basin, are consistent with hypotheses of polygenetic waters in the region (Porowski 2014, 2015).

Finally, I/S measurements modelled for two wells in the hydrothermal basin, used to calibrate the volume of water released from clay dehydration, fitted with measurements (Środoń et al. 2006) by considering two potassium contents (K^+=0.00052 and K^+=0.000052; concentration in molarity; see figure inset). While the Banska IG1 well could be explained by a potassium content that diminished with depth, measured

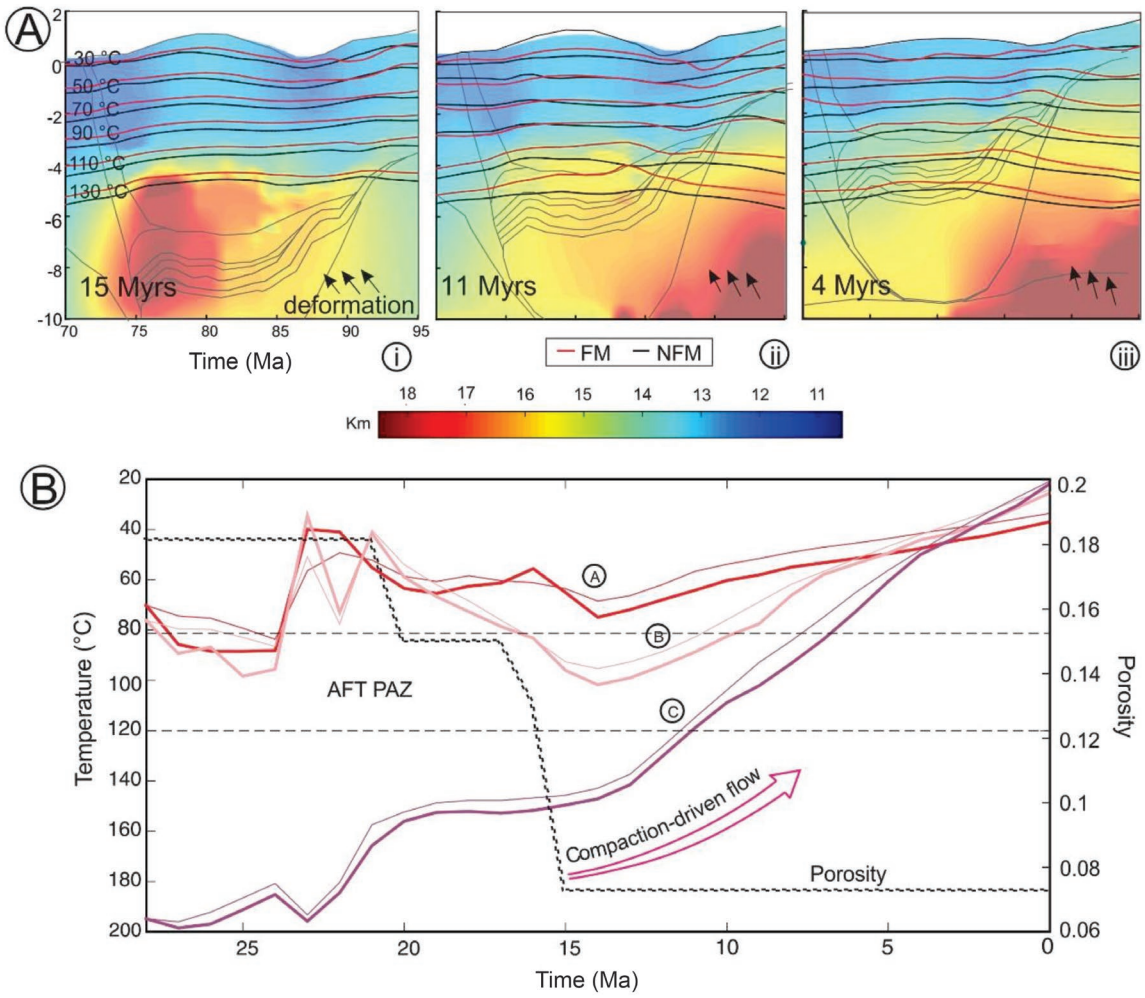

Fig. 5. A — Hydrological evolution of the Podhale Basin. Colour scale represents piezometric head. Isotherms from FM (fluid model) are shown as red lines, whereas isotherms from the NFM (no fluid model) are shown in black. **B** — Time temperature paths of selected samples. Bold and thin lines represent results from the FM and NFM, respectively. Porosity expressed in fractional units.

values at Furmanowa IG1 well were satisfactorily reproduced by running a model with a constant, low K+ availability. It is worth mentioning that our thermo-hydrological exercise yielded the pattern shown by well data, despite the fact that (a) clay kinetics is still being understood; therefore, the Huang et al. (1993) model constitutes a simplification (see Cuadros 2006), and (b) potassium content in the area has not yet been constrained, and thus the model can be further enhanced by incorporating a depth-dependent K-law for each well. Taking all the above into consideration, the I/S results casted by our model satisfactorily predict clay diagenesis.

Apatite Fission Track (AFT) and Apatite U–Th/He (AHe) modelling

Figure 4 shows measured and simulated thermochronological ages considering models with (FM) and without (NFM) fluid circulation through porous media. In general, even though the correlation and misfit between modelled and measured ages varies through the study area, the FM shows a better fit than the NFM, specially at the flysch strata of Podhale's basin (see Figs. 1 and 4), where the difference between the NFM and measurements becomes significant (~20 Ma).

Toward the recharge area (i.e., the Tatra Mts., see location in Figs. 1, 3 and 4), the correlation between measured and modelled AFT ages is relatively good (Fig. 4), with most samples in this region (C region in Fig. 4) exhibiting modelled ages in agreement with measured data. No appreciable difference is seen here between the FM and the NFM scenarios. At the basin (i.e., toward the discharge area), we point that despite the fact that measured the large dispersion, the difference between the FM modelled and sampled ages is less than 5 Ma (Fig. 4). We can also note that the farther the samples crop from the area of low permeability (Tatra Mts.), the greater the mismatch between NFM and the measured ages, especially in the vicinity of PKB (i.e., structural impermeable barrier). The only measured AHe age (12.7±2.2 Ma), obtained from

Eocene strata next to such structural barrier (PKB), is also better explained by FM. We could therefore conclude that even though some samples are not precisely reproduced by FM, our model clearly shows a better adjustment than those that do not incorporate the fluid influence. Our results, evidence the fluid-driven heating (and thermal-resetting) present in the Podhale Basin, which might apply to other scenarios and geological settings.

Discussion

Thermochronological modelling

The results yielded by our model incorporating fluid flow, supported by different thermal, hydrological and mineralogical calibrations; suggest that low-temperature thermochronological ages, like fluid movement, are hydrologically-conditioned. This constitutes the main conclusion from our work, as previous studies (Mora et al. 2015; Castelluccio et al. 2015) only considered cooling ages to be dependant on kinematic histories and boundary conditions (e.g., basal temperature). Furthermore, this contribution, which likely represents the first effort to couple hydrological and thermochronological modelling in structurally complex scenarios, puts forward a more comprehensive view of a geological system and the processes within a thrust belt and associated basins. We expand on the aforementioned along the following lines.

The apparent similarity of the two modelling scenarios at the Tatra Mts. could be attributed to the poor hydrological properties (primary porosity and permeability) of the granitic rocks that compose the mega anticline. Since no secondary porosity (or permeability) was considered in our models, the poorly hydraulically-conductive basement of the Tatra Mts. anticline would not have been significantly affected by water circulation (see Table 2). This is clearly shown by our output data, i.e., both models (FM and NFM) reproduce similar results. Nonetheless, it is worth noticing that considering secondary porosity or permeability might yield older (and better fitted) ages for the model with Darcian circulation (FM), as the presence of cold waters that enter into the hydrological system could bend down the isotherms (Husson & Moretti 2002). In addition, thermal conductivity would be reduced by the increase of rock water content (see equation 4), which would restrain heat transference from below and thus, yield cooler temperatures. All the aforementioned would lead to a lower thermal gradient, causing our model results (19 °C/km) to better fit the observed value (14 °C/km). The NFM, in contrast, could only reduce such age difference by considering different basal heat flows or modifying the tectonic and structural reconstructions (basically burial and exhumation, which are directly related to sedimentation, uplift and erosion). Nevertheless, such considerations are likely more difficult to fit given that a new tectonic proposal in the IWC should correlate with different others geological observations in the region (see Castelluccio et al. 2015).

The discharge area (Podhale Basin), in turn, shows a shortly-spaced, drastic variation in measured AFT ages (see Fig. 4, at ~30 Ma and between 69 and 72 km), which has constituted a very complex modelling enterprise (see Castelluccio et al. 2015). Considering the sampling distances and structural features (sub-horizontal strata involved in deformation), such age distributions cannot be associated only with thrusting reconstruction strategies and/or erosion. Examination of the NFM AFT ages corroborates such fact, as the values yielded for the three northernmost samples (52.15 Ma, 33.28 Ma and 20.42 Ma) lie far from the measured AFT ages (39.4 Ma, 12.4 Ma and 7.6 Ma, respectively). In contrast, misfit for the FM remains roughly constant, irrespective of the distance to the Tatra Mts., suggesting that thermal effects of fluid flow are fairly represented by our numerical effort. The differences between the modelled ages (FM and NFM) in the basin highlight the major influence of the circulation of groundwater to the north, since towards this region the results are separated more than in other areas. In agreement with hydrological observations (Chowaniec & Poprawa 1998; Operacz & Chowaniec 2018), this could relate to the presence of PKB (impermeable barrier), which hampers fluid movement outside Podhale Basin and channelizes upward flows at the northern part of the section. Such flows were not accounted for by NFM, thus yielding large errors.

Hydrological evolution of Podhale Basin and its influence on the thermal state

Our modelling results suggest that the hydrologic state (piezometric head) changed at peace with tectonic deformation (see Fig. 5), influencing in turn the thermal state and thermochronological ages. Figure 5A shows the hydrologic and thermal evolution since 15 Ma, after the main structural shortening took place and the Podhale Basin was formed (see Castelluccio et al. 2015). The connection between the hydrological architecture of the basin and the resultant thermal field is unveiled, confirming previous assertions on regard of thermochronological modelling.

Erosion of Oligocene strata from the late Miocene to present (from Fig. 5A: i–iii) would have caused the topographic-driven flows to migrate southward, to the Tatra Mts. (see changes in the piezometric head gradient along the relief line across the basin, Fig. 5A: i–iii and Fig. 5B). Contemporaneously with such migration, water derived from deformationally-driven mechanical compaction, related to the most intense period of tectonic shortening (6.5 km/Ma shortening rate from 18 to 15 Myrs, Castelluccio et al. 2015) was incorporated to the fluid budget of the basin. This deformation stage produced a remarkable increment in the lithostatic loading, driving localized pore-pressure gradients and consequent upwelling flows that are still present in the area (e.g., piezometric potential below the Banska well in Fig. 3). Another interesting paleohydrological scenario, strongly connected with the tectonic history, was observed between 15 and 11 Ma (Fig. 5A: i–ii). A major fall of the piezometric heads at 8–4 km depth

(see red area in Fig. 5A: i to become yellow in Fig. 5A: ii), likely related to water sourced driven by porosity reduction in this zone, increases locally the vertical heat flow and, consequently, alters the thermochronological results.

Figure 5B shows the time–temperature (t–T) evolution of three selected samples across the study area (A, B and C; see Fig. 4), which represent three different hydrological and deformed areas, and allowed us to support our conclusions on the strong control of water on the thermal field and cooling age modelling. FM (thick curves) yields paths with higher temperatures than NFM. The samples extracted from the Tatra anticline (e.g., C), toward the discharge area, exhibit no major variation between the FM and the NFM simulations, ascribed to an almost equal residence time within the AFT partial annealing zone (AFT PAZ, see Fig. 5B). In contrast, residence time (and depth) for the samples collected from the Podhale Basin (A and B) differs remarkably in the two models. The ages estimated using the FM are subject to a greater degree of thermal resetting than those using the NFM. This difference between t–T paths is related to the hydrological–thermal coupling considered in the FM. In fact, this effect is clear between the 18–15 Ma lapse (Fig. 5B), where most compaction of Oligocene strata occurs (most significant episode of porosity reduction), driving dewatering and hot fluid upwelling since then. The strong influence of fluids on temperature is also observed at 11 Ma (Fig. 5A). Our FM reproduces the 110 °C and 130 °C isotherms at shallower positions (~1 km) than the NFM (compare thick and thin curves in Fig. 5B, respectively), related to the vertical movement of groundwater. As the fluid perturbation dissipates (because shortening and compaction also reduce, see stage at 4 Ma, Fig 5A: iii)), the difference between the two models narrows, generating equidistant isotherms every ~500 m, and similar t–T paths (see Fig. 5B).

While our models (particularly FM) demonstrate the strong control of fluid flows on temperature and cooling ages, smectite-to-illite modelling allowed us to assert that no major overpressure was produced by clay dehydration. This, however, contrasts with previous studies, which suggest that the diagenetic process seems to play a major role on groundwater generation and overpressuring (Saffer et al. 2008; Saffer & Tobin 2011; Lauer & Saffer 2015). In addition to hydrology, as stated in the model calibration above, I/S modelling allowed us to corroborate our thermochronological analysis. For example, the Banska IG1 well (located toward the discharge area close to the PKB) exhibits a complex I/S evolution pattern, where two model scenarios are needed to reproduce the observed smectite fractions (see Inset in Fig. 3, i.e., K^+=0.00052 for the upper part and K^+=0.000052 for the lower one). On the other hand, I/S data from Furmanowa PIG1 well (located near the recharge area, Tatra Mts.) does not exhibit major fluctuations along the well and can be reproduced running a model with low K^+ availability. Similar to the thermochronological results, toward the recharge area (to the Tatra Mts.) the I/S evolution is simpler than toward those regions affected by groundwater circulation (Podhale Basin).

Model limitations and further insights

With regard to the numerical model, we point out that the applicability of the model is restricted to geological environments where piezometric head assumptions can be conservatively stated. Such is the case of the ICTB, where the documented structural reconstructions and present-day geology suggest a fully water-saturated system (see Castelluccio et al. 2015). Whenever such hypothesis may not be safely taken (like for instance, on the rest of the thrust belt aimed by this work, which led us to restrict the study region accordingly), the code applicability may be challenged.

In our case study, secondary porosity and permeability were not addressed, even though fluid circulation has been suggested to operate under an interconnected system of fissures rather than within the pore space (Chowaniec 2004; Sowiżdżał & Semyrka 2016). However, secondary permeability and hydraulic conductivity measurements are still not available for underground rocks and, for a kinematic modelling, it cannot be predicted spatially and temporally. Future efforts will for sure benefit of the new forthcoming data, as the study region is not only of economic interest but also has been addressed with different research objectives.

Finally, we point out that our results open a question mark on previous computations, where basal heat flow changes, lithospheric thermal properties or/and burial and exhumation have been the only drivers to fit measured and modelled cooling ages (e.g., Dávila & Carter 2013; Parks & McQuarrie 2019). Even though such an approach has been valuable deciphering thermal histories for many situations (Braun 2016; Margirier et al. 2018, among others), it may not be appropriate for some cases; as shown here for the Inner Carpathians of Poland. Undoubtedly, the model requires additional improvement (reproduction of AFT ages can be certainly enhanced, shear stresses added; to begin with). However, along with what we consider the nucleus of this work, it calls for a reappraisal of the heating processes that take part on the cooling history of sediments, and thus, of their consequent thermochronological ages. Could different conclusions be derived from previous numerical efforts if they were now reproduced considering water influence? Could increment of basal heat flow, usually the preferred mechanism to promote thermal-resetting or hotter environments, be replaced by ascent of hot fluids from below? On the other hand, could cooler systems be reproduced by, instead of the commonly called for low-geothermal gradients, a water-filled porosity space? We recall that the presence of water-saturated fractures not only reduces substantially the mixed thermal conductivity of rocks (rocks and void spaces, see Eq. 4), but also prevents heat transference, given that heat capacity of water is among the highest in nature. All the aforementioned implies that water presence can promote different thermal effects. On one hand, upwelling of water that has already been heated (for instance, as an effect of head-induced downward circulation), aids vertical heat flow and temperature increment. Such is the case evidenced by this work. On the other hand, because of porosity and water heat

capacity, the presence of non-heated (i.e shallow) water can retard heat transference from the underground, thus cooling down the system. Similar observations have already been made for subduction regimes in respect to heat convection from metamorphic fluids (e.g., Peacock 1987, 1990). From all the above; the combination of hydrological effects, or, even more, a superposition of them, could have major implications on thermochronological modelling and its stemming interpretations (as disclosed by this work). Posterior efforts will constrain the answers to the questions here posed, casting some light on this issue.

Conclusions

By considering groundwater flow through fluid-saturated pore space, this new version of the Fetkin program (developed and provided by Ecopetrol, see Almendral et al. 2015) successfully couples hydrological and thermal modelling, providing thus an unprecedented view on numerical thermochronological efforts, so far mostly focused on burial and exhumation processes. Our results disclose the linking between pore-pressure and thermal processes, suggesting that as long as thermochronological calculations are concerned, the interplay between them should be considered. Most prominent thermal and hydrological features of IWC are satisfactorily reproduced, yielding considerably better results than the model without Darcian circulation. Regarding model applicability, we note that the model here considered requires assessment of the water table through time, which may represent a barrier to overcome for some future case-studies. Such future works will not only enhance numerical aspects of the code, but also, our understanding of the processes involved in fold and thrust belts.

Acknowledgments: We thank CONICET, SECyT-UNC and FONCyT that fund our researches in Argentina. We also appreciate reviewers and editorial work that allowed improving the original version of our manuscript.

References

Almendral A., Robles W., Parra M., Mora A., Ketcham R.A. & Raghib M. 2015: FetKin: Coupling kinematic restorations and temperature to predict thrusting, exhumation histories, and thermochronometric ages. Coupling Kinematic Restorations and Temperature. *AAPG Bulletin* 99, 1557–1573. https://doi.org/10.1306/07071411112

Anczkiewicz A.A., Środoń J. & Zattin M. 2013: Thermal history of the Podhale Basin in the internal Western Carpathians from the perspective of apatite fission track analyses. *Geologica Carpathica* 64, 141–151. https://doi.org/10.2478/geoca-2013-0010

Andreucci B. 2013: Thermochronology of the Polish and Ukrainian Carpathians. *Ph.D. thesis*, Padua, Padua research, 1–144.

Bear J. & Verruijt A. 2012:Modelling groundwater flow and pollution (Vol. 2). *Springer Science & Business Media.*

Braun J. 2003: Pecube: A new finite-element code to solve the 3D heat transport equation including the effects of a time-varying, finite amplitude surface topography. *Computers & Geosciences* 29, 787–794. https://doi.org/10.1016/S0098-3004(03)00052-9

Braun J. 2016: Strong imprint of past orogenic events on the thermochronological record. *Tectonophysics* 683, 325–332. https://doi.org/10.1016/j.tecto.2016.05.046

Braun J. & Willett S.D. 2013: A very efficient O (n), implicit and parallel method to solve the stream power equation governing fluvial incision and landscape evolution. *Geomorphology* 180, 170–179. https://doi.org/10.1016/j.geomorph.2012.10.008

Burchart J. 1972: Fission-track age determination of accessory apatite from the Tatra Mountains, Poland. *Earth and Planetary Science Letters* 15, 418–422. https://doi.org/10.1016/0012-821X(72)90041-6

Castelluccio A., Benedetta A., Zattin M., Ketcham R, Jankowski L., Mazzoli S. & Szaniawski R. 2015: Coupling sequential restoration of balanced cross sections and low-temperature thermochronometry: The case study of the Western Carpathians. *Lithosphere* 7, 367–378. https://doi.org/10.1130/L436.1

Chowaniec J. 2004: Hydrogeological properties of the Podhale flysch (Central Western Carpathians, Poland) in the light of studies on water storage capacity. *Geologica Carpathica* 55, 77–81.

Chowaniec J. 2009: Hydrogeology study of the western part of the Polish Carpathian. *Biuletyn Panstwowego Instytutu Geologicznego* 734, 1–98.

Chowaniec J. & Poprawa D. 1998: Thermal waters of the Polish part of the Carpathians. *Przeglad Geologiczny* 46, 770–774.

Cobbold P.R., Mourgues R. & Boyd K. 2004: Mechanism of thin-skinned detachment in the Amazon Fan: assessing the importance of fluid overpressure and hydrocarbon generation. *Marine and petroleum geology* 21, 1013–1025. https://doi.org/10.1016/j.marpetgeo.2004.05.003

Coussens J., Woodman N., Upton P., Menzies C.D., Janku-Capova L., Sutherland R. & Teagle D.A. 2018: The significance of heat transport by shallow fluid flow at an active plate boundary: The Southern Alps, New Zealand. *Geophysical Research Letters* 45, 10–323. https://doi.org/10.1029/2018GL078692

Cuadros J. 2006: Modelling of smectite illitization in burial diagenesis environments. *Geochimica et Cosmochimica Acta* 70, 4181–4195. https://doi.org/10.1016/j.gca.2006.06.1372

Danišík M., Kohút M., Evans N.J. & Mcdonald B.J. 2012: Eo-Alpine metamorphism and the 'mid-Miocene thermal event in the Western Carpathians (Slovakia): new evidence from multiple thermochronology. *Geological Magazine* 149, 158–171. https://doi.org/10.1017/S0016756811000963

Dávila F.M. & Carter A. 2013: Exhumation history of the Andean broken foreland revisited. *Geology* 41, 443–446. https://doi.org/10.1130/G33960.1

Davis D., Suppe J. & Dahlen F.A. 1983: Mechanics of fold-and-thrust belts and accretionary wedges. *Journal of Geophysical Research: Solid Earth* 88, 1153–1172. https://doi.org/10.1029/JB088iB02p01153

Deming D. 1994: Fluid flow and heat transport in the upper continental crust. *Geological Society, London, Special Publications* 78, 27–42. https://doi.org/10.1144/GSL.SP.1994.078.01.04

Evans J.P., Forster C.B. & Goddard J.V. 1997: Permeability of fault-related rocks, and implications for hydraulic structure of fault zones. *Journal of structural Geology* 19, 1393–1404. https://doi.org/10.1016/S0191-8141(97)00057-6

Forster C. & Smith L. 1989: The influence of groundwater flow on thermal regimes in mountainous terrain: a model study. *Journal of Geophysical Research: Solid Earth* 94, 9439–9451. https://doi.org/10.1029/JB094iB07p09439

Gallagher K. 2012: Transdimensional inverse thermal history modelling for quantitative thermochronology. *Journal of Geophysical Research: Solid Earth* 117. https://doi.org/10.1029/2011JB008825

Ge S. & Garven G. 1992: Hydromechanical modelling of tectonically driven groundwater flow with application to the Arkoma foreland basin. *Journal of Geophysical Research: Solid Earth* 97, 9119–9144. https://doi.org/10.1029/92JB00677

Georgieva V., Gallagher K., Sobczyk A., Sobel E.R., Schildgen T.F., Ehlers T.A. & Strecker M.R. 2019: Effects of slab-window, alkaline volcanism, and glaciation on thermochronometer cooling histories, Patagonian Andes. *Earth and Planetary Science Letters* 511, 164–176. https://doi.org/10.1016/j.epsl.2019.01.030

Gonzalez-Penagos F., Moretti I., France-Lanord C. & Guichet X. 2014: Origins of formation waters in the Llanos foreland basin of Colombia: geochemical variation and fluid flow history. *Geofluids* 14, 443–458. https://doi.org/10.1111/gfl.12086

Hantschel T. & Kauerauf A.I. 2009: Fundamentals of basin and petroleum systems modelling. *Springer Science & Business Media*.

Hardebol N.J., Callot J.P., Bertotti G. & Faure J.L. 2009: Burial and temperature evolution in thrust belt systems: Sedimentary and thrust sheet loading in the SE Canadian Cordillera. *Tectonics* 28. https://doi.org/10.1029/2008TC002335

Hók J., Šujan M. & Šipka F. 2014: Tektonické členenie Západných Karpát – prehľad názorov a nový prístup. *Acta Geologica Slovaca* 6, 135–143.

Huang W.L., Longo J.M. & Pevear D.R. 1993: An experimentally derived kinetic model for smectite-to-illite conversion and its use as a geothermometer. *Clays and Clay Minerals* 41, 162–177. https://doi.org/10.1346/CCMN.1993.0410205

Husson L. & Moretti I. 2002: Thermal regime of fold and thrust belts – an application to the Bolivian sub Andean zone. *Tectonophysics* 345, 253–280. https://doi.org/10.1016/S0040-1951(01)00216-5

Jessop A.M. & Majorowicz J.A. 1994: Fluid flow and heat transfer in sedimentary basins. *Geological Society, London, Special Publications* 78, 43–54. https://doi.org/10.1144/GSL.SP.1994.078.01.05

Kępińska B. 2004: The Podhale geothermal system and heating project – an overview. In: International Geothermal Days Poland 2004, Zakopane, September 13–17, 1–16.

Kępińska B. 2006: Thermal and hydrothermal conditions of the Podhale geothermal system. *Studia, Rozprawy, Monografie IGSMiE PAN w Krakowie* 135, 1–112 (in Polish with English summary).

Ketcham R.A. 2005: Forward and inverse modelling of low-temperature thermochronometry data. *Reviews in mineralogy and geochemistry* 58, 275–314. https://doi.org/10.2138/rmg.2005.58.11

Králiková S., Vojtko R., Sliva Ľ., Minár J., Fügenschuh B., Kováč M. & Hók J. 2014: Cretaceous–Quaternary tectonic evolution of the Tatra Mts. (Western Carpathians): Constraints from structural, sedimentary, geomorphological, and fission track data. *Geologica Carpathica* 65, 307–326. https://doi.org/10.2478/geoca-2014-0021

Lauer R.M. & Saffer D.M. 2015: The impact of splay faults on fluid flow, solute transport, and pore pressure distribution in subduction zones: A case study offshore the Nicoya Peninsula, Costa Rica. *Geochemistry, Geophysics, Geosystems* 16, 1089–1104. https://doi.org/10.1002/2014GC005638

López D.L. & Smith L. 1996: Fluid flow in fault zones: influence of hydraulic anisotropy and heterogeneity on the fluid flow and heat transfer regime. *Water Resources Research* 32, 3227–3235. https://doi.org/10.1029/96WR02101

Łuszczak K., Persano C., Braun J. & Stuart F.M. 2017: How local crustal thermal properties influence the amount of denudation derived from low-temperature thermochronometry. *Geology* 45, 779–782. https://doi.org/10.1130/G39036.1

Maheľ M. 1981: Island character of Klippen Belt; Vahicum – continuation of Southern Penninicum in West Carpathians. *Geologický Zborník – Geologica Carpathica* 32, 293–305.

Margirier A., Braun J., Robert X. & Audin L. 2018: Role of erosion and isostasy in the Cordillera Blanca uplift: Insights from landscape evolution modelling (northern Peru, Andes). *Tectonophysics* 728, 119–129. https://doi.org/10.1016/j.tecto.2018.02.009

Marynowski L. & Gawęda A. 2005: Correlation between biomarkers and thermal maturity of the organic matter from the Paleogene sedimentary rocks of the Podhale trough. *Mineralogical Society of Poland, Special Papers* 25, 329–332.

Marynowski L., Gawęda A. & Kępińska B. 2005: Thermal Regime of the Podhale Geothermal System (Poland) in the Light of Organic Matter Maturation and Other Research Methods. In: Proceedings World Geothermal Congress 2005, Antalya, Turkey. https://www.academia.edu/19235921

Mora A., Casallas W., Ketcham R.A., Gomez D., Parra M., Namson J., Stockli D.F., Vazquez A.A., Robles W. & Ghorbal B. 2015: Kinematic restoration of contractional basement structures using thermokinematic models: A key tool for petroleum system modelling. *AAPG Bulletin* 99, 1575–1598. https://doi.org/10.1306/04281411108

Nemčok M., Schamel S. & Gayer R. 2009: Thrustbelts: Structural architecture, thermal regimes and petroleum systems. *Cambridge University Press*, 1–556.

Operacz A. & Chowaniec J. 2018: Perspectives of geothermal water use in the Podhale Basin according to geothermal step distribution. *Geology, Geophysics and Environment* 44, 379–389. https://doi.org/10.7494/geol.2018.44.4.379

Parks V.M.B. & McQuarrie N. 2019: Kinematic, flexural, and thermal modelling in the Central Andes: Unravelling age and signal of deformation, exhumation, and uplift. *Tectonophysics* 766, 302–325. https://doi.org/10.1016/j.tecto.2019.06.008

Peacock S.M. 1987: Thermal effects of metamorphic fluids in subduction zones. *Geology* 15, 1057–1060. https://doi.org/10.1130/0091-7613(1987)15%3C1057:TEOMFI%3E2.0.CO;2

Peacock S.M. 1990: Numerical simulation of metamorphic pressure-temperature-time paths and fluid production in subducting slabs. *Tectonics* 9, 1197–1211. https://doi.org/10.1029/TC009i005p01197

Pešková I., Vojtko R., Starek D. & Sliva Ľ. 2009: Late Eocene to Quaternary deformation and stress field evolution of the Orava region (Western Carpathians). *Acta Geologica Polonica* 59, 73–91.

Pomianowski P. 1988: Thermal anomalies above the contact zone of the Pieniny Klippen Belt and the Podhale Flysch. *Przegląd Geologiczny* 36, 94–97(in Polish with English abstract).

Porowski A. 2014: Chemical and Isotopic Characteristics of Thermal Waters in the Carpathian Region, South Poland: Implication to the Origin and Resources. In: Balderer W., Porowski A., Idris H. & LaMoreaux J. (Eds.): Thermal and Mineral Waters. *Environmental Earth Sciences*, 73–89. https://doi.org/10.1007/978-3-642-28824-1_7

Porowski A. 2015: Geothermometric and isotopic studies of dehydration waters: implications for thermal conditions in the Central Carpathian Synclinorium, SE Poland. *Environmental Earth Sciences* 74, 7539–7553. https://doi.org/10.1007/s12665-015-4631-0

Roberson H.E. & Lahann R.W. 1981: Smectite to illite conversion rates: effects of solution chemistry. *Clays and Clay Minerals* 29, 129–135. https://doi.org/10.1346/CCMN.1981.0290207

Saffer D.M. & Tobin H.J. 2011: Hydrogeology and mechanics of subduction zone forearcs: Fluid flow and pore pressure. *Annual Review of Earth and Planetary Sciences* 39, 157–186. https://doi.org/10.1146/annurev-earth-040610-133408

Saffer D.M., Underwood M.B. & McKiernan A.W. 2008: Evaluation of factors controlling smectite transformation and fluid production in subduction zones: Application to the Nankai Trough. *Island Arc* 17, 208–230. https://doi.org/10.1111/j.1440-1738.2008.00614.x

Samuel O. & Fusán O. 1992: Reconstruction of subsidence and sedimentation of Central Carpathian Paleogene. *Západné Karpaty, Séria Geológia* 16, 7–46.

Sanchez F., Barrea A., Dávila F.M. & Mora A. 2021:Fetkin-hydro, a new thermo-hydrological algorithm for low-temperature thermochronological modelling. *Geoscience Frontiers* 12, 101074. https://doi.org/10.1016/j.gsf.2020.09.005

Śmigielski M., Stuart F.M., Krzywiec P., Persano C., Sinclair H.D., Pisaniec K. & Sobień K. 2012:. Neogene exhumation of the Northern Carpathians revealed by low temperature thermochronology. In: EGU General Assembly Conference Abstracts, 12063.

Sokołowski J. 1993: Geothermal resources in Poland and possibility of their utilization in environmental protection. *Exploration Geology, Geosynoptics and Geothermal Energy* 5, 67–80.

Sowiżdżał A. & Semyrka R. 2016: Analyses of permeability and porosity of sedimentary rocks in terms of unconventional geothermal resource explorations in Poland. *Geologos* 22, 149–163. https://doi.org/10.1515/logos-2016-0015

Spinelli G.A., Saffer D.M. & Underwood M.B. 2006: Hydrogeologic responses to three-dimensional temperature variability, Costa Rica subduction margin. *Journal of Geophysical Research: Solid Earth* 111. https://doi.org/10.1029/2004JB003436

Środoń J., Kotarba M., Biroň A., Such P., Clauer N. & Wójtowicz A. 2006: Diagenetic history of the Podhale-Orava Basin and the underlying Tatra sedimentary structural units (Western Carpathians): evidence from XRD and K-Ar of illite-smectite. *Clay Minerals* 41, 751–774. https://doi.org/10.1180/0009855064130217

Świerczewska A. 2005: The interplay of the thermal and structural histories of the Magura Nappe (Outer Carpathians) in Poland and Slovakia. *Mineralogia Polonica* 36, 91–144.

Van Keken P.E., Kiefer B. & Peacock S.M. 2002: High-resolution models of subduction zones: Implications for mineral dehydration reactions and the transport of water into the deep mantle. *Geochemistry, Geophysics, Geosystems* 3, 1–20. https://doi.org/10.1029/2001GC000256

Voigt S., Wagreich M., Surlyk F., Walaszczyk I., Uličný D., Čech S., Voigt T., Wiese F., Wilmsen M., Niebuhr B. & Reich M. 2008: Cretaceous. *Geology of Central Europe* 6, 923–997. https://doi.org/10.1144/CEV2P.3

Vojtko R., Tokárová E., Sliva Ľ. & Pešková I. 2010: Reconstruction of Cenozoic paleostress fields and revised tectonic history in the northern part of the Central Western Carpathians (the Spišská Magura and Východné Tatry Mountains). *Geologica Carpathica* 61, 211–225. https://doi.org/10.2478/v10096-010-0012-5